

POTENTIATION OF THE TRANSIENT RECEPTOR POTENTIAL VANILLOID 1 CHANNEL CONTRIBUTES TO PRURITOGENESIS IN A RAT MODEL OF LIVER DISEASE

Majedeline Belghiti¹, Judith Estévez-Herrera¹, Carla Giménez-Garzó¹, Alba González-Usano¹, Carmina Montoliu², Antonio Ferrer-Montiel³, Vicente Felipo¹, Rosa Planells-Cases^{1,4}

¹Centro de Investigación Príncipe Felipe, Valencia, Spain

²Instituto de Biología Molecular y Celular, Universidad Miguel Hernández, Elche, Spain

³Fundación Investigación Hospital Clínico de Valencia, INCLIVA, Valencia, Spain

⁴Leibniz-Institut für Molekulare Pharmakologie (FMP) and Max-Delbrück-Centrum für Molekulare Medizin (MDC), Berlin, Germany

*Running title: TRPV1 in cholestatic pruritus

To whom correspondence should be addressed: Rosa Planells-Cases, Leibniz-Institut für Molekulare Pharmakologie (FMP) and Max-Delbrück-Centrum für Molekulare Medizin (MDC), Robert-Roessle-Str. 10. 13125 Berlin, Germany. Tel.: +49-30-9406-2965. Fax: +49-30-9406-2960
Email: planells-cases@fmp-berlin.de

Keywords: protease activated receptor, peripheral sensitization, capsaicin receptor

Background: The etiology and neurophysiology of generalized pruritus associated with liver disease remain unknown.

Results: Rats with bile duct ligation displayed enhanced scratching and thermal hyperalgesia dependent on PAR₂ activation and TRPV1 potentiation.

Conclusion: Pruritus and hyperalgesia in BDL-rats is associated with neuroinflammation and involves PAR₂-induced TRPV1 sensitization.

Significance: Pharmacological modulation of PAR₂ and/or TRPV1 emerges as a potential therapeutic approach for liver pruritus refractory to conventional treatments.

SUMMARY

Persistent pruritus is a common disabling dermatologic symptom associated with different etiologic factors. These include primary skin conditions, as well as neuropathic, psychogenic or systemic disorders like chronic liver disease. Defective clearance of potential pruritogenic substances that activate itch-specific neurons innervating

the skin is thought to contribute to cholestatic pruritus. However, because the underlying disease-specific pruritogens and itch-specific neuronal pathways and mechanism(s) are unknown, symptomatic therapeutic intervention often leads to no or only limited success. In the current study, we aimed to first validate rats with bile duct ligation (BDL) as a model for hepatic pruritus, and then to evaluate the contribution of inflammation, peripheral neuronal sensitization, and specific signaling pathways and subpopulations of itch-responsive neurons to scratching behavior and thermal hypersensitivity. Chronic BDL rats displayed enhanced scratching behavior and thermal hyperalgesia indicative of peripheral neuroinflammation. BDL-induced itch and hypersensitivity involved a minor contribution of histaminergic/serotonergic receptors, but significant activation of PAR₂ receptors, prostaglandin PGE₂ formation and potentiation of TRPV1 channel activity. The sensitization of DRG nociceptors in BDL rats was associated with increased surface

expression of PAR₂ and TRPV1 proteins and an increase in the number of PAR₂- and TRPV1-expressing peptidergic neurons together with a shift of TRPV1 receptor expression to medium-sized DRG neurons. These results suggest that pruritus and hyperalgesia in chronic cholestatic BDL rats are associated with neuroinflammation and involves PAR₂-induced TRPV1 sensitization. Thus, pharmacological modulation of PAR₂ and/or TRPV1 may be a valuable therapeutic approach for patients with chronic liver pruritus refractory to conventional treatments.

INTRODUCTION

Chronic pruritus is a common, seriously debilitating symptom that can arise from dermatologic disorders, but often also appears in other disease states as a secondary symptom (1). For instance, chronic itch has been associated with a wide variety of pathologies such as malignancy, or hematologic, infectious, neuropsychiatric, metabolic and systemic disorders. Patients with end-stage renal and hepatic diseases often present with pruritus that might result from diminished renal or hepatic clearance of pruritogenic substances.

The origin of hepatic pruritus remains poorly understood. The pathological accumulation of specific pruritogens is thought to directly or indirectly activate unmyelinated C-fibers that innervate the skin (2,3). However, both the identity of disease-specific pruritogen(s) and the neuronal pathways and mechanism(s) involved in pruritus are highly controversial. For instance, although bile salts and other cholephiles are traditionally assumed to be major pruritogens, no correlation exists between pruritus intensity and either serum biomarkers for cholestasis or with the course of the disease (1,4). It is widely accepted that other substances like the well-known pruritogens histamine and serotonin (5-HT), which are released from mast cells, or endogenous opioids, that are liberated from immune cells, may accumulate in hepatic pruritus and activate sensory neurons (5,6). Whereas 5-HT and opioid receptor antagonists have therapeutic potential in a subset of cholestasis patients, antihistaminics have proven ineffective (7). Recently, increased serum levels of autotaxin

and lysophosphatidic acid (LPA) were proposed as mediators in human cholestatic pruritus (8-11). In addition to inducing histamine release from mast cells, LPA impinges on proinflammatory transcriptional factors, promotes cytokine production and platelet activation (12) and enhances cytokine-induced COX-2 expression (13). Indeed, high serum levels of pro-inflammatory cytokines like IL-31 (14) or Tumor Necrosis Factor α (TNF- α) and interleukin 6 (IL-6), that are both associated with liver fibrosis (15,16), might also contribute to itch.

TRPV1 (Transient Receptor Potential Vanilloid 1) is a polymodal receptor channel that conducts cations (preferentially Ca²⁺) in response to either the irritant compound capsaicin, or to extracellular acidic pH and to noxiously high temperatures ($\geq 43^{\circ}\text{C}$). Pharmacological and genetic abrogation of TRPV1 function in rodents significantly reduces pain in acute and chronic inflammatory animal models (17,18). Whereas TRPV1 channel activity is low under normal conditions, mediators released from injured cells and activated immune cells during inflammation potentiate TRPV1 activity through activation of G-protein coupled receptors (GPCRs), thereby leading to sensitization of nociceptive neurons (19).

Besides being a pain sensor, TRPV1 may also be an itch integrator of both histaminergic (2,20) and some non-histaminergic pruritogens like serotonin or iquimimod (2,21). Binding of pruritogens to their receptors, whose identity is often unclear, can trigger distinct and specific intracellular signaling pathways that can activate and potentiate TRPV1 function (2,22). Hence TRPV1 may be a common downstream effector in the itch signaling pathway. Indeed, most noxious stimuli can produce pain and/or itch, depending on how and where they are applied (23). Recently, certain subsets of TRPV1-expressing C-fibers with specific sensory modalities have been reported to distinctly respond to different pruritogens like histamine, 5-HT or chloroquine (2,21,24). Nevertheless, our understanding of the mechanisms involved in pruritus signaling by TRPV1-expressing neurons remains limited.

To our knowledge, no previous study has addressed the neuronal mechanism(s) underlying pruritus associated with cholestatic liver disease,

a dynamic and complex condition leading to inflammation, liver fibrosis and eventually cirrhosis. We hypothesized that a Wistar rat model with chronic bile duct ligation (BDL) (16) may display increased scratching bouts and provide a model of cholestatic pruritus. We investigated the involvement of specific pathways and subpopulations of itch-responsive neurons by pharmacological intervention with selective antagonists and by immunohistochemistry. In particular, because neurogenic inflammation in chronic BDL rats (16,25) may contribute to pruritus through TRPV1 sensitization (26,27), we investigated the role of TRPV1 as a final integrator in the itch signaling pathway.

Here, we show that Wistar BDL rats exhibit augmented scratching accompanied by peripheral sensitization of primary afferents as revealed by thermal hyperalgesia. Both symptoms showed an early onset that correlated with an increase in both, serum biomarkers for cholestasis and proinflammatory cytokines. Whereas histamine/serotonin pathways only play a minor role in the scratching and thermal hyperalgesia phenotype of our rat model, our results demonstrate an involvement of Protease Activated Receptor-2 (PAR₂) activation, peripheral inflammation and TRPV1 potentiation. Hence targeting the recruitment or modulation of PAR₂ or TRPV1 may be useful therapeutic strategies to treat chronic itch and neuroinflammation in liver disease patients.

EXPERIMENTAL PROCEDURES

Animals—Male Wistar rats (200-250 g) were obtained from Charles River, France. Experimental procedures were approved by the Ethics Committee and met EU guidelines for care and management of experimental animals. BDL rats were operated as described (16). Control rats were sham operated. Behavioral studies started 48 h after surgery and only when no signs of pain or distress were apparent. Pharmacological treatments were initiated 3 weeks after surgery and their effects were evaluated until up to three months later.

Drugs and reagents—The contribution of different signaling pathways was assessed by subcutaneous (sc) administration of cyproheptadine (20 mg/kg) (28), intraperitoneal

(ip) injection of naloxone HCl (20 mg/kg), gabexate mesylate (10 mg/kg, sc), FSLLRY-NH₂ (200 µg, sc), ibuprofen (20 mg/kg ip), meloxicam (1 mg/kg, sc), capsazepine (2 mg/kg, sc) (29), DD04107 or a lipopeptide containing the scrambled (Scr) sequence of DD04107 (3 mg/kg, sc). Drugs were prepared immediately before use in 0.9% NaCl from a stock solution. Control groups received the corresponding vehicle. Cyproheptadine, protease and opioid antagonists were administered 30 min, and other drugs 60 min, before behavioral tests.

All drugs were from Sigma (St. Louis, MO) unless otherwise stated. PAR₂ agonist (PAR₂-AP), a negative retropeptide control (PAR₂-RP) and FSLLRY-NH₂ (PAR₂-Antg) were from Bachem (Bubendorf, Switzerland), meloxicam (Metacam®) from Boehringer Ingelheim, gabexate mesylate from Tocris (Bristol, UK) and palmitoylated DD04107 and the scrambled control lipopeptide were synthesized by DiverDrugs (Gavà, Spain).

Primary antibodies used were anti- α -CGRP (Novus Biol., Littleton, CO), anti-PAR₂ (Santa Cruz Biotech, Santa Cruz, CA) and anti-TRPV1 (Alomone, Jerusalem, Israel), NF200 and monoclonal anti- β -actin (Sigma). Secondary antibodies were from Jackson (West Grove, PA). **Behavioral analysis**—Rats were acclimatized in a measuring cage for 30 min, followed by videotaping of scratching behavior for 30 min or 1 h. Spontaneous scratching was quantified by counting the number of scratches of any region of the body performed by forepaws or hindpaws. For Hargreaves' Plantar Test a standard apparatus (Ugo Basile, Italy) was used that automatically measured the paw withdrawal latency (PWL) to a thermal radiant stimulus (30). To avoid tissue injury in refractory animals, stimulation was automatically terminated after 32 s. PWL was determined before and after drug or vehicle treatment in BDL and sham control rats. Data are presented as mean \pm SEM with a minimum of six animals per group.

Determination of cholestasis and inflammation—Serum bilirubin (BR), alkaline phosphatase (AP), glutamic oxaloacetic transaminase (GOT) and glutamic pyruvic transaminase (GPT) were determined by standard techniques and prostaglandin PGE₂ by ELISA (GE Healthcare, Sweden).

Ca²⁺ imaging in primary cultures of dorsal root ganglion (DRG) neurons—Primary adult sham and BDL DRGs cultures were established as described [24]. Fluorescence measurements were performed after approximately 12h *in vitro* in paired BDL and sham DRG cultures as in (31). To investigate PAR₂ modulation of TRPV1 activity, cells were exposed 5 min to PAR₂ agonist (AP), antagonist (Antg) or vehicle, followed by a 10 s pulse with 100 nM capsaicin (32).

Biotin labeling of surface TRPV1 and PAR₂ proteins—Dissociated DRG neurons from Sham and BDL-operated rats were surface biotinylated with sulfo-NHS-SS-Biotin (Pierce, Rockford, IL) and processed as described (33). Biotinylated proteins were isolated with streptavidin agarose, resolved by SDS-PAGE and detected with the following antibodies and dilutions: TRPV1 (1:1000), PAR₂ (1:100) and β -actin (1:200). Immunoblots were digitized and quantified. The absence of contaminating intracellular proteins in membrane fractions was verified by labeling of actin.

Immunofluorescent staining of DRG neurons and measurement of size of neuronal somata—Rats were over-anesthetized and then transcardially perfused with saline and then with 4% paraformaldehyde (PFA) (pH 7.4). DRGs were quickly removed, post-fixed, and then placed in sucrose solution. 8 μ m sections were co-incubated with anti-TRPV1 (1:1000) and FITC-IB4 (1:50) or one of the following antibodies: anti-NF200 (1:1000), anti- α -CGRP (1:300), anti-GRP (1:500) or anti-PAR₂ (1:100) overnight at 4°C. Cy3- or Alexa 488-tagged secondary antibodies were used in 1:200 dilutions for 1 h at 22°C. Sections were then washed 3 times for 10 min in PBS and mounted. Controls for double-labeling experiments included imaging with both green and red filters in the presence of only one primary antibody and/or by omission of all primary antibodies. Settings for each channel were initially adjusted as to avoid bleeding through. Images were taken on a Leica DM5000B epifluorescence microscope fitted with a digital camera. When comparing different samples, identical settings were used.

The areas of TRPV1 positive (TRPV1+) neurons and DRG neuronal markers were analyzed by

tracing the soma perimeter on a computer screen in a calibrated image and using ImageJ software (NIH, Bethesda, MD). Calculated areas were plotted against the percentage of total TRPV1+ neurons. More than 5 sections per animal, 3 pairs of rats, and >1000 total neurons per phenotype were analyzed.

Statistical analysis—Results are expressed as mean \pm SEM. The non-parametric test Mann-Whitney was used for paired comparisons. Between groups, one-way ANOVA was followed by Tukey test. Differences were considered significant when *P \leq 0.1, **P<0.01 and ***P<0.001.

Additional methods and materials are described in *Suppl. Experimental Procedures*.

RESULTS

Chronic BDL rats displayed increased scratching mediated by PAR₂ signaling and neuroinflammation.

We evaluated whether spontaneous scratching behavior was increased in Wistar BDL rats, an animal model that leads to jaundice, inflammation and cirrhosis (16). Cumulative spontaneous scratching bouts (SSB) during 1 h observation periods were recorded in BDL- and sham-operated animals at different time points. As shown in Fig. 1A, BDL rats exhibited a significant (\approx 2-fold) elevation in the number of SSBs (SSB = 59 \pm 4, n=12, in BDL compared to 39 \pm 4, n=8, in sham rats) 48 h after surgery, a behavior that persisted for at least 3 months. Cholestasis was evident from increased serum bilirubin and AP levels, as well as from elevated levels of hepatic injury markers GOT and GPT (table I). Similarly, pro-inflammatory interleukin IL-6 was elevated in BDL sera, as shown previously (16).

To determine the involvement of different molecular pathways in enhanced scratching, we first administered the mixed histaminergic/serotonergic antagonist cyproheptadine (Cypr). This procedure slightly decreased spontaneous scratching bouts in BDL rats (SSB = 66 \pm 4 compared to 94 \pm 5 with vehicle, n=7) (Fig. 1B). In contrast, scratching bouts were markedly reduced when BDL rats were treated with the systemic opioid receptor antagonist naloxone

HCl (NaHCl) (SSB = 22 ± 5 versus 84 ± 6 with saline, $n=7$) (Fig. 1B).

Besides histamine and endogenous opioids (33), also trypsin, chymase and other proteases are released during inflammation by immune cells (34). To assess the involvement of proteases in the scratching behavior, we administered the specific Lima bean trypsin inhibitor, the serine protease inhibitor gabexate mesylate and the PAR₂ receptor antagonist, FSLLRY-NH₂ into BDL and sham-operated rats. Importantly, all three antagonists produced a marked decrease in scratching behavior. Thus, for instance, the Lima bean trypsin inhibitor reduced the SSB in BDL rats to 38 ± 7 (compared to 86 ± 10 with saline ($n=7$)) (data not shown). Similarly, as illustrated in Fig. 1C, the serine protease inhibitor gabexate mesylate reduced SSB to 16 ± 1 compared to 89 ± 2 with saline injection ($n=7$), and the PAR₂ antagonist FSLLRY-NH₂ diminished SSB to 38 ± 11 versus 85 ± 4 with saline treatment ($n=7$). Since all three inhibitors are predicted to prevent activation of PAR₂, the scratching behavior in BDL rats may be mediated, at least in part, by PAR₂ activation.

Chronic BDL rats display increased thermal hyperalgesia.

Primary afferents responding to serotonin and PAR₂ activation are polymodal C-fibers that also respond to noxious stimuli like mustard oil and capsaicin (34). Moreover, PAR₂ has been implicated in both pruritus (3,28,34-36) and hyperalgesia (37,38). We therefore asked whether hepatic pruritus in Wistar BDL rats might be accompanied by altered nociceptive thermal responses. Indeed, the paw withdrawal latency (PWL) from a hot source was significantly shorter in BDL rats than in control animals. For instance, 3 weeks after surgery, PWL in BDL rats was reduced to 9.0 ± 0.4 s ($n=21$) compared to 15.6 ± 0.5 s in controls ($n=19$). The thermal hypersensitivity in BDL rats remained constantly increased over the time of our analysis (Fig. 2A).

We next evaluated the role of histamine/serotonin, endogenous opioids and protease pathways on thermal hypersensitivity. Whereas the histaminergic/serotonergic antagonist Cypr did not interfere with the withdrawal latency in Wistar chronic BDL rats, a single dose of NaHCl or of the protease

inhibitors gabexate methyle or of PAR₂-Antg significantly attenuated BDL thermal hyperalgesia (Fig. 2B and 2C). Interestingly, administration of either gabexate mesylate or of PAR₂-Antg reverted PWL values close to those of control rats.

PAR₂ activation triggers inflammatory responses through phospholipase PLA₂ activation and arachidonic acid release (39). We therefore used ibuprofen, a cyclooxygenase COX-1/COX-2 inhibitor, and the preferential COX-2 inhibitor meloxicam (data not shown) to analyze the role of eicosanoids in the itch response. Ibuprofen administration reduced scratching bouts by about 50% (Fig. 3A). Furthermore, as expected, heat hypersensitivity in BDL rats was reversed both by ibuprofen (Fig. 3B) and by the selective COX-2 antagonist meloxicam (data not shown). Importantly, the ibuprofen-induced change in serum levels of PGE₂ correlated remarkably well with the observed behavioral index (Fig. 3A and 3C). These experiments therefore suggest that prostanoids are involved in liver disease-associated pruritus and that thermal hyperalgesia in chronic BDL rats is mostly mediated by a PAR₂ signaling pathway.

TRPV1 contributes to itch and thermal hyperalgesia in BDL rats.

Because activated PAR₂ may modulate neurogenic inflammation and increase nociceptor excitability by potentiating TRPV1 activity (40), we determined the contribution of TRPV1 sensitization to pruritus. Systemic administration of the TRPV1 antagonist capsazepine (CPZ) to BDL- and sham-operated rats produced a significant attenuation in spontaneous scratching bouts in BDL, but not in control rats (BDL: SSB = 21 ± 2 compared to 86 ± 5 in vehicle, $n=6$; sham-operated: SSB = 47 ± 5 compared to 46 ± 5 in vehicle, $n=6$) (Fig. 4A). Likewise, CPZ blocked thermal hyperalgesia in chronic BDL rats (PWL = 17.3 ± 0.6 s compared to 10.7 ± 0.7 s in vehicle-treated BDL rats, $n=9$) (Fig. 4B).

Enhanced TRPV1 activity may arise either from increased intrinsic channel activity and/or from enhanced plasma membrane expression (19,40). To assess whether regulated exocytotic plasma membrane insertion of TRPV1 contributed to the inflammatory sensitization of TRPV1 in BDL rats, we evaluated the

antinociceptive and antipruritic activities of DD04107, a lipopeptide known to interfere with vesicle fusion in nociceptors (40). It is based on SNAP25 peptide sequence and is thought to compete with SNAP25 for its incorporation into a SNARE complex that is needed for exocytosis in neurons. As illustrated in Fig. 4A, systemic administration of DD04107 significantly decreased the scratching bouts in BDL rats as compared with the administration of a lipopeptide containing the scrambled DD04107 sequence (Scr) ($SSB = 20 \pm 4$ versus 73 ± 8 , $n=6$, respectively). Similarly DD04107 selectively attenuated the thermal hypersensitivity in chronic BDL rats (Fig. 4B). Hence, recruitment of TRPV1 to the membrane of nociceptor terminals likely contributes importantly to enhanced scratching behavior in BDL rats.

Acutely dissociated DRG neurons from BDL rats display PAR₂ upregulation and increased TRPV1 activity.

Since pharmacological inhibition of PAR₂ and TRPV1 significantly reduced scratching and thermal hyperalgesia in BDL rats, we asked whether altered PAR₂ and/or TRPV1 function might be detected in acutely dissociated DRG neurons from BDL rats. To prevent serial dilution of proinflammatory substances, cells were only cultured for about 12 h, with no change in culture media. Paired nociceptor cultures from BDL- and sham-operated rats were tested by exposing them for 5 min to either vehicle (Veh), 100 μ M PAR₂ agonist (AP) or antagonist (Antg), always followed by a test pulse of the TRPV1 agonist capsaicin (Caps; 100 nM). Because the TRPV1 channel is highly permeable to Ca²⁺, we used the ratiometric Ca²⁺-sensitive indicator dye FURA-2 to assess capsaicin responses. As shown in Fig. 5, under control (Veh) conditions, BDL DRG neurons displayed both significantly increased magnitudes of individual responses (Fig. 5A and 5B) and a larger percentage of responding neurons (Fig. 5C). Interestingly, previous activation of PAR₂ with PAR₂-AP produced a >2-fold increase in the percentage of capsaicin-responsive neurons in sham cultures, reaching a level that was close to that observed with vehicle in BDL neurons (Fig. 5C). Hence, even when inflammatory agents might be partially or completely diluted, BDL DRG nociceptors

appeared submaximally activated, suggesting a long-lasting modification of TRPV1 activity. As negative control, PAR₂-RP had no effect. Moreover, PAR₂ receptor silencing by transfection of paired BDL and control neurons with a specific PAR₂ small interfering RNA (siRNA), previously shown to strongly reduce PAR₂ protein levels in nociceptor cultures, significantly produced concomitant reduced capsaicin responses in both types of cultures (supplemental Fig. 1A-D). The augmented PAR₂ activity in BDL DRGs was associated with an increase in PAR₂-receptor immunoreactivity in DRGs (Fig. 6A) and an approximately 2-fold enhanced recruitment of PAR₂ receptors to the plasma membrane as revealed by immunodetection of surface biotinylated fractions (Fig. 6B). Altogether, these results indicate that nociceptors of BDL rats are sensitized by increased PAR₂-signaling.

To better characterize TRPV1 potentiation in BDL rats, we evaluated the average magnitude of Ca²⁺ influx and the percentage of responding nociceptors from paired BDL- and sham-DRG cultures at different agonist concentrations (from 1 nM to 5 μ M capsaicin). Over the entire concentration range, TRPV1-mediated Ca²⁺ influx into BDL neurons was increased about 2-fold compared to controls (Figs. 5D and 5E). The half-maximal effective capsaicin concentration (EC₅₀) for evoking intracellular [Ca²⁺] increases was 12 ± 2 nM in BDL neurons, versus 360 ± 30 nM for sham cultures. A transcription-independent, ≈ 2 -fold increase in TRPV1 protein levels was observed in DRG homogenates from BDL rats compared to controls (Supplemental Fig. 2). Importantly, similar to enhanced PAR₂ surface expression in BDL nociceptors, a significant translocation of TRPV1 receptor channels to the plasma membrane was found by surface protein biotinylation (Fig 6B). This data was further confirmed by immunocytochemistry of nonpermeabilized live BDL and sham-neurons using a TRPV1 antibody that recognizes an extracellular epitope (Supplemental Fig. 3). The percentage of capsaicin-responsive neurons was also notably higher in BDL DRG cultures (Fig. 5F). Thus, whereas $\approx 40\%$ of sham neurons was activated by 1 μ M capsaicin, this percentage increased up to $\approx 80\%$ in BDL cultures. These results were bolstered by immunohistochemistry

that revealed a robust increase in the number of TRPV1-expressing neurons in BDL DRG sections (Fig. 6B).

We next examined whether the increased percentage of capsaicin-responsive neurons correlated with a shift of TRPV1 expression to a specific DRG subpopulation. DRG cryosections were colabeled for TRPV1 and calcitonin gene-related peptide (CGRP) or isolectin B4 (IB4), two markers commonly used to identify peptidergic and non-peptidergic C-fibers, respectively, and for neurofilament NF200 to identify medium and large size myelinated A-fibers. Fig. 6C displays examples of DRG sections from control and BDL rats (left and right columns, respectively) labeled for TRPV1 (red) and different DRG markers (green), and double-labeled neurons (yellow). Remarkably, whereas the percentage of cells immunoreactive to TRPV1 and IB4 remained unaltered, the proportion of peptidergic neurons coexpressing TRPV1 and CGRP (TRPV1⁺CGRP⁺) was significantly increased in BDL rats (36.7±4.5% compared to 25.4±3.9% in sham control, *P<0.1).

Agreeing with previous work [37], area histograms showed that TRPV1 was mainly expressed in small diameter neurons. TRPV1⁺CGRP⁺ neurons clustered in the smaller group (areas <600 μm²). Notably, the number of TRPV1⁺CGRP⁺ was significantly increased in BDL rats (Fig. 6C and 6D). A second major difference was noticed within medium-size neurons (800-1,200 μm²) (Fig. 6E), which probably correspond to somata of A-fibers. The percentage of TRPV1⁺NF200⁺ neurons was increased about 3-fold in BDL rats as compared to sham-operated rats (20±5 and 6±2%, respectively). Taken together, these findings indicate that both an upregulation of PAR₂ and TRPV1 protein expression in nociceptors, as well as a potentiation of their activity, underlie the scratching behavior observed in this model of chronic liver disease.

DISCUSSION

In this study, we have established an animal model for pruritus associated with cholestasis. Our work suggests that histamine/serotonin pathways play only a minor role in hepatic

pruritogenesis. By contrast, stimulation of PAR₂ receptors, that might be activated by mast cell tryptase released in inflammatory processes, lead to the potentiation of the capsaicin TRPV1 receptor channel activity. This activation, which also leads to thermal hyperalgesia, involves several mechanisms, including increased cellular expression, plasma membrane residence, and intrinsic channel activity.

We used a model of cholestatic liver fibrosis based on bile duct ligation in Wistar rats, a procedure that eventually leads to cirrhosis and to hepatic encephalopathy (16,25,41). We found that BDL rats display increased spontaneous scratching indicative of itch, a common dermatologic symptom in chronic liver disease. Increased scratching emerged shortly after surgery and lasted for up to three months, the latest time point investigated. Unlike previous models of acute cholestasis by bile duct resection in rodents that display decreased nociception (5,42), our model resulted in increased thermal hyperalgesia. This difference cannot be accounted for by differences in the duration of cholestasis, as we observed thermal hyperalgesia already 48 hours after surgery. However, differences between rat strains in nociception thresholds (43,44) could well account for these differences. Importantly, our observation of thermal hyperalgesia in BDL rats perfectly fits to the upregulation and sensitization of the heat-sensitive TRPV1 channel which we have demonstrated in this work.

Patients with cholestasis and itch display signs of peripheral neuroinflammation as reflected by increased numbers of dermal mast cells (45). Furthermore, increased mast cell degranulation has been reported in animals with chronic biliary obstruction (46). However, in spite of intensive investigation, the mediators and neuronal mechanisms involved in cholestatic pruritus remain still unresolved. Recently, autaxin and LPA levels have been correlated with itch intensity in cholestatic patients (47). LPA induces histamine release from mast cells (48). However, histamine seems to play only a minor role in cholestatic pruritus both in patients (49) and in our rat model.

On the other hand, autaxin is highly expressed in submucosal mast cells also containing chimase and tryptase (50). Tryptase and other proteases,

released during mast cell degranulation, do not only serve to cleave many substrates involved in inflammation and wound repair, but also potently activate protease-activated PAR₂ receptors (51). Indeed, we found a significant activation of PAR₂ receptors, enhanced downstream prostaglandin PGE₂ formation, and potentiation of TRPV1 channel activity. DRG nociceptors in BDL rats displayed increased overall expression of PAR₂ and TRPV1 proteins, an increased number of PAR₂- and TRPV1-expressing peptidergic neurons, and a shift of TRPV1 receptor expression to medium-sized DRG neurons. This changed pattern of TRPV1 expression has been found in animal models of hyperalgesia associated with acute and chronic inflammation (52,53), supporting our conclusion that inflammation plays an important role in cholestatic pruritus.

Protease- and PAR₂-mediated signaling pathways have been implicated in neurogenic inflammation, in certain types of generalized pruritus (28,54), and also in hyperalgesia (37,38). Notably, patients refer cholestatic pruritus as an *irritation* that cannot be relieved by scratching (4), a sensation that could be well accounted for by peripheral neuronal sensitization. An activation of the Mas-related G protein-coupled receptor MgrprC11, rather than of PAR₂, was recently proposed as underlying the scratching behavior elicited by PAR₂-AP agonist or trypsin administration (24). On the other hand, mucunain, the active ingredient of cowhage, is known to induce itch and a burning sensation through activation of PAR₂ and PAR₄ (55). Moreover, other reports stressed a pivotal role of PAR₂ in skin conditions such as in dry-skin itch (35) and in atopic dermatitis (56,57). The importance of PAR₂ activation in our model was not only confirmed pharmacologically by antagonist administration, but also by specific silencing of the PAR₂ receptor in primary BDL nociceptor cultures.

PAR₂ activation has been reported to modulate the expression and ion channel activity of TRPV1 (37,38). We therefore evaluated the magnitude of TRPV1 activity and its modulation by PAR₂ in nociceptor cultures. Under basal conditions, both the percentage of capsaicin-responding neurons and the individual cellular response to the TRPV1 agonist capsaicin were \approx 4-fold higher in

BDL nociceptors. TRPV1 sensitization by PAR₂ activation appeared to reach near-maximal levels in BDL rats, since the percentage of TRPV1+ neurons derived from those rats was not further increased when challenged with PAR₂ agonist. These results suggest an upregulation of PAR₂-signaling in BDL nociceptors which was corroborated by Western blots and immunohistochemistry.

Although TRPV1 protein levels in BDL nociceptors were only increased 2-fold, the TRPV1 channel activity elicited by the agonist capsaicin was increased about 30-fold. In addition to increasing transcription and/or translation, pro-inflammatory stimuli can sensitize TRPV1 by several additional mechanisms which either lead to a fast, acute decrease of the activation threshold by receptor phosphorylation, or to an increased residence of the protein at the cell surface. The functional coupling of PAR₂ to TRPV1 through PKC ϵ - and PKA-mediated phosphorylation of TRPV1 has been well documented (38). The effect of an *in vivo* application of an inhibitor previously demonstrated to block regulated exocytosis of TRPV1 in DRG nociceptor cultures (19,40) now suggested an important contribution of increased plasma membrane insertion of TRPV1 in the genesis of both pruritus and thermal hyperalgesia.

In summary, our work indicates that activation of PAR₂ signaling, presumably by inflammatory release of proteases from cutaneous mast cells found in close proximity to nerve terminals, sensitizes nociceptors by augmenting the expression and activity of neuronal TRPV1 channels. The presence of additional pro-inflammatory mediators like autaxin, LPA, IL-6, PGE₂ and TNF α may further enhance nociceptor sensitization and/or mast cell degranulation, thus contributing to the persistence of a pruritogenic state. PAR₂ receptors and TRPV1 channels may be interesting therapeutic targets for developing compounds that attenuate chronic systemic pruritus arising from liver disease or possibly from other systemic disorders.

Acknowledgements– The authors thank Drs F. J. Rodríguez-Jiménez and V. Moreno-Manzano (CIPF) for help with qRT-PCR experiments.

REFERENCES

1. Weisshaar, E., Kucenic, M. J., and Fleischer, A. B., Jr. (2003) *Acta Derm Venereol Suppl (Stockh)*, 5-32
2. Imamachi, N., Park, G. H., Lee, H., Anderson, D. J., Simon, M. I., Basbaum, A. I., and Han, S. K. (2009) *Proc Natl Acad Sci U S A* **106**, 11330-11335
3. Steinhoff, M., Neisius, U., Ikoma, A., Fartasch, M., Heyer, G., Skov, P. S., Luger, T. A., and Schmelz, M. (2003) *J Neurosci* **23**, 6176-6180
4. Bergasa, N. V., Mehlman, J. K., and Jones, E. A. (2000) *Baillieres Best Pract Res Clin Gastroenterol* **14**, 643-655
5. Nelson, L., Vergnolle, N., D'Mello, C., Chapman, K., Le, T., and Swain, M. G. (2006) *J Hepatol* **44**, 1141-1149
6. Weisshaar, E., Ziethen, B., Rohl, F. W., and Gollnick, H. (1999) *Exp Dermatol* **8**, 254-260
7. Glasova, H., and Beuers, U. (2002) *J Gastroenterol Hepatol* **17**, 938-948
8. Kremer, A. E., Martens, J. J., Kulik, W., Rueff, F., Kuiper, E. M., van Buuren, H. R., van Erpecum, K. J., Kondrackiene, J., Prieto, J., Rust, C., Geenes, V. L., Williamson, C., Moolenaar, W. H., Beuers, U., and Oude Elferink, R. P. (2012) *Gastroenterology* **139**, 1008-1018
9. Kremer, A. E., Martens, J. J., Kulik, W., Williamson, C., Moolenaar, W. H., Kondrackiene, J., Beuers, U., and Elferink, R. P. J. O. (2009) *Acta Derm-Venereol* **89**, 702-702
10. Kremer, A. E., Martens, J. J., Kulik, W., Williamson, C., Moolenaar, W. H., Kondrackiene, J., Beuers, U., and Elferink, R. P. J. O. (2010) *J Hepatol* **52**, S1-S1
11. Kremer, A. E., Martens, J. J., Kulik, W., Williamson, C., Moolenaar, W. H., Kondrackiene, J., Beuers, U., and Elferink, R. P. O. (2009) *Hepatology* **50**, 376a-376a
12. van Meeteren, L. A., and Moolenaar, W. H. (2007) *Prog Lipid Res* **46**, 145-160
13. Nochi, H., Tomura, H., Tobo, M., Tanaka, N., Sato, K., Shinozaki, T., Kobayashi, T., Takagishi, K., Ohta, H., Okajima, F., and Tamoto, K. (2008) *J Immunol* **181**, 5111-5119
14. Takaoka, A., Arai, I., Sugimoto, M., Honma, Y., Futaki, N., Nakamura, A., and Nakaïke, S. (2006) *Exp Dermatol* **15**, 161-167
15. Barak, V., Selmi, C., Schlesinger, M., Blank, M., Agmon-Levin, N., Kalickman, I., Gershwin, M. E., and Shoefeld, Y. (2009) *J Autoimmun* **33**, 178-182
16. Jover, R., Rodrigo, R., Felipe, V., Insausti, R., Saez-Valero, J., Garcia-Ayllon, M. S., Suarez, I., Candela, A., Compan, A., Esteban, A., Cauli, O., Auso, E., Rodriguez, E., Gutierrez, A., Girona, E., Erceg, S., Berbel, P., and Perez-Mateo, M. (2006) *Hepatology* **43**, 1257-1266
17. Garcia-Martinez, C., Humet, M., Planells-Cases, R., Gomis, A., Caprini, M., Viana, F., De La Pena, E., Sanchez-Baeza, F., Carbonell, T., De Felipe, C., Perez-Paya, E., Belmonte, C., Messeguer, A., and Ferrer-Montiel, A. (2002) *Proc Natl Acad Sci U S A* **99**, 2374-2379
18. Caterina, M. J., and Julius, D. (2001) *Annu Rev Neurosci* **24**, 487-517
19. Planells-Cases, R., Garcia-Sanz, N., Morenilla-Palao, C., and Ferrer-Montiel, A. (2005) *Pflugers Arch* **451**, 151-159
20. Shim, W. S., Tak, M. H., Lee, M. H., Kim, M., Kim, M., Koo, J. Y., Lee, C. H., Kim, M., and Oh, U. (2007) *J Neurosci* **27**, 2331-2337
21. Kim, S. J., Park, G. H., Kim, D., Lee, J., Min, H., Wall, E., Lee, C. J., Simon, M. I., Lee, S. J., and Han, S. K. *Proc Natl Acad Sci U S A* **108**, 3371-3376
22. Biro, T., Toth, B. I., Marincsak, R., Dobrosi, N., Geczy, T., and Paus, R. (2007) *Biochim Biophys Acta* **1772**, 1004-1021
23. Ross, S. E. (2011) *Curr Opin Neurobiol* **21**, 880-887
24. Liu, Q., Weng, H. J., Patel, K. N., Tang, Z., Bai, H., Steinhoff, M., and Dong, X. *Sci Signal* **4**, ra45
25. Montoliu, C., Piedrafita, B., Serra, M. A., del Olmo, J. A., Urios, A., Rodrigo, J. M., and Felipe, V. (2009) *Journal of clinical gastroenterology* **43**, 272-279
26. Seeliger, S., Derian, C. K., Vergnolle, N., Bunnett, N. W., Nawroth, R., Schmelz, M., Von Der Weid, P. Y., Buddenkotte, J., Sunderkotter, C., Metzger, D., Andrade-Gordon, P., Harms, E., Vestweber, D., Luger, T. A., and Steinhoff, M. (2003) *Faseb J* **17**, 1871-1885
27. Namer, B., Carr, R., Johaneck, L. M., Schmelz, M., Handwerker, H. O., and Ringkamp, M. (2008) *J Neurophysiol* **100**, 2062-2069
28. Costa, R., Marotta, D. M., Manjavachi, M. N., Fernandes, E. S., Lima-Garcia, J. F., Paszcuk, A. F., Quintao, N. L., Juliano, L., Brain, S. D., and Calixto, J. B. (2008) *Br J Pharmacol* **154**, 1094-1103
29. Perkins, M. N., and Campbell, E. A. (1992) *Br J Pharmacol* **107**, 329-333
30. Hargreaves, K., Dubner, R., Brown, F., Flores, C., and Joris, J. (1988) *Pain* **32**, 77-88
31. Lainez, S., Valente, P., Ontoria-Oviedo, I., Estevez-Herrera, J., Camprubi-Robles, M., Ferrer-Montiel, A., and Planells-Cases, R. (2010) *Faseb J* **24**, 1958-1970
32. Amadesi, S., Cottrell, G. S., Divino, L., Chapman, K., Grady, E. F., Bautista, F., Karanjia, R.,

- Barajas-Lopez, C., Vanner, S., Vergnolle, N., and Bunnett, N. W. (2006) *J Physiol* **575**, 555-571
33. Sanz-Salvador, L., Andres-Borderia, A., Ferrer-Montiel, A., and Planells-Cases, R. (2012) *J Biol Chem* **287**, 19462-19471
34. Akiyama, T., Merrill, A. W., Carstens, M. I., and Carstens, E. (2009) *J Neurosci* **29**, 6691-6699
35. Akiyama, T., Merrill, A. W., Zanutto, K., Carstens, M. I., and Carstens, E. (2009) *J Pharmacol Exp Ther* **329**, 945-951
36. Tsujii, K., Andoh, T., Ui, H., Lee, J. B., and Kuraishi, Y. (2009) *J Pharmacol Sci* **109**, 388-395
37. Amadesi, S., Nie, J., Vergnolle, N., Cottrell, G. S., Grady, E. F., Trevisani, M., Manni, C., Geppetti, P., McRoberts, J. A., Ennes, H., Davis, J. B., Mayer, E. A., and Bunnett, N. W. (2004) *J Neurosci* **24**, 4300-4312
38. Dai, Y., Moriyama, T., Higashi, T., Togashi, K., Kobayashi, K., Yamanaka, H., Tominaga, M., and Noguchi, K. (2004) *J Neurosci* **24**, 4293-4299
39. van der Merwe, J. Q., Ohland, C. L., Hirota, C. L., and MacNaughton, W. K. (2009) *J Pharmacol Exp Ther* **329**, 747-752
40. Camprubi-Robles, M., Planells-Cases, R., and Ferrer-Montiel, A. (2009) *Faseb J* **23**, 3722-3733
41. Rodrigo, R., Cauli, O., Gomez-Pinedo, U., Agusti, A., Hernandez-Rabaza, V., Garcia-Verdugo, J. M., and Felipe, V. (2010) *Gastroenterology* **139**, 675-684
42. Hasanein, P., Parviz, M., Keshavarz, M., Javanmardi, K., Allahtavakoli, M., and Ghaseminejad, M. (2007) *European journal of pharmacology* **554**, 123-127
43. Miura, T., Okazaki, R., Yoshida, H., Namba, H., Okai, H., and Kawamura, M. (2005) *J Pharmacol Sci* **97**, 429-436
44. Banik, R. K., Sato, J., Yajima, H., and Mizumura, K. (2001) *Neurosci Lett* **299**, 21-24
45. Twycross, R., Greaves, M. W., Handwerker, H., Jones, E. A., Libretto, S. E., Szepietowski, J. C., and Zylicz, Z. (2003) *Qjm* **96**, 7-26
46. Clements, W. D., O'Rourke, D. M., Rowlands, B. J., and Ennis, M. (1994) *Agents and actions* **41 Spec No**, C30-31
47. Kremer, A. E., Dijk, R. V., Leckie, P., Schaap, F. G., Kuiper, E. M., Mettang, T., Reiners, K. S., Raap, U., Buuren, H. R., Erpecum, K. J., Davies, N. A., Rust, C., Engert, A., Jalan, R., Elferink, R. P., and Beuers, U. (2012) *Hepatology*
48. Hashimoto, T., Ohata, H., Momose, K., and Honda, K. (2005) *Pharmacology* **75**, 13-20
49. Mela, M., Mancuso, A., and Burroughs, A. K. (2003) *Aliment Pharmacol Ther* **17**, 857-870
50. Mori, K., Kitayama, J., Aoki, J., Kishi, Y., Shida, D., Yamashita, H., Arai, H., and Nagawa, H. (2007) *Virchows Archiv : an international journal of pathology* **451**, 47-56
51. Steinhoff, M., Buddenkotte, J., Shpacovitch, V., Rattenholl, A., Moormann, C., Vergnolle, N., Luger, T. A., and Hollenberg, M. D. (2005) *Endocrine reviews* **26**, 1-43
52. Amaya, F., Oh-hashii, K., Naruse, Y., Iijima, N., Ueda, M., Shimosato, G., Tominaga, M., Tanaka, Y., and Tanaka, M. (2003) *Brain Res* **963**, 190-196
53. Yu, L., Yang, F., Luo, H., Liu, F. Y., Han, J. S., Xing, G. G., and Wan, Y. (2008) *Molecular pain* **4**, 61
54. Ui, H., Andoh, T., Lee, J. B., Nojima, H., and Kuraishi, Y. (2006) *European journal of pharmacology* **530**, 172-178
55. Reddy, V. B., Iuga, A. O., Shimada, S. G., LaMotte, R. H., and Lerner, E. A. (2008) *J Neurosci* **28**, 4331-4335
56. Yosipovitch, G., and Papoiu, A. D. (2008) *Curr Allergy Asthma Rep* **8**, 306-311
57. Briot, A., Deraison, C., Lacroix, M., Bonnart, C., Robin, A., Besson, C., Dubus, P., and Hovnanian, A. (2009) *J Exp Med* **206**, 1135-1147

FOOTNOTES

¹This work was supported by grants from the Ministry of Science and Innovation (BFU2009-08346 to AF-M; SAF2008-00062 to VF and SAF2007-63193 to RP-C), the Consolider-Ingenio 2010 program (CSD2008-00005 to AF-M, VF and RP-C), and la Generalitat Valenciana (Prometeo-2010-046 to AF-M; AP-092/09, Prometeo-2009-027 and ACOMP2010-220 to VF).

²The abbreviations used are: AP, Alkaline Phosphatase; BDL, Bile Duct Ligation; CGRP, Calcitonin Gene-Related Peptide; COX, cyclooxygenase; DRG, Dorsal Root Ganglion; IB4, GOT, Glutamic Oxaloacetic Transaminase; GPT, Glutamic Pyruvic Transaminase; Isolectin B4; LPA, Lysophosphatidic acid; NF200, Neurofilament 200kDa; PAR₂, Protease Activated Receptor-2; PWL, Paw withdrawal latency; siRNA, small interfering RNA; SSBSpontaneous Scratching Bouts; TRPV1, Transient Receptor Potential Vanilloid 1.

FIGURE LEGENDS

Figure 1. Effect of the blockade of histamine/serotonin-, opioid-, protease- and PAR₂-activated pathways in the enhanced scratching behavior of a rat model with Bile Duct Ligation (BDL). (A) Time course of cumulative spontaneous scratching bouts per hour in BDL (●) and sham-operated (○) control rats after surgery (n=8-12). (B) Effect of the mixed His/5-HT antagonist cyproheptadine (Cypr) and the systemic opioid antagonist naloxone HCl (Nal.HCl) on the spontaneous scratching bouts per hour. (C) Spontaneous scratching bouts after administration of the protease inhibitor gabexate mesylate (Gabex.Mes) and PAR₂ antagonist (PAR₂-Antg) recorded during first 30 min. V= vehicle, T= treatment. n=6-9 animals. Each data point represents mean ± SEM. (*P<0.0, **P<0.01, ***P<0.001 Mann Whitney test).

Figure 2. Effect of the blockade of histamine/serotonin-, opioid-, protease- and PAR₂-activated pathways on the increased thermal hyperalgesia in a rat model with Bile Duct Ligation (BDL) (A) Time course of paw withdrawal latency from a heat source in BDL (●) and sham-operated (○) control rats after surgery (n=8-12). (B) Effect of the mixed His/5-HT antagonist cyproheptadine (Cypr) and the systemic opioid antagonist naloxone HCl (Nal.HCl) and (C) of the protease inhibitor gabexate mesylate (Gabex.Mes) and PAR₂ antagonist (PAR₂-Antg) on thermal sensitivity. V= vehicle, T= treatment. n=6-9 animals. Each data point represents mean ± SEM. (*P<0.1, ***P<0.001, Mann Whitney test).

Figure 3. Role of COX-1/COX-2 in spontaneous scratching and thermal hyperalgesia in BDL rats. (A) Time course of scratching bouts per hour and (B) of the paw withdrawal latency from a heat source of BDL and sham-operated rats. Vehicle controls and animals treated with a single dose (20 mg/kg, ip.) of the COX-1/COX-2 inhibitor ibuprofen (Ibu) are compared. (C) Serum PGE₂ levels after the single ibuprofen administration in both BDL and sham operated rats. Each point represents the mean with SEM. of n=6.

Figure 4. Enhanced pruritus and thermal hyperalgesia in BDL rats is attenuated by TRPV1 inhibition and by blockade of TRPV1 membrane translocation. (A) Effect on spontaneous scratching bouts per hour and (B) on paw withdrawal latency from a heat source of the selective TRPV1-inhibitor capsazepin (CPZ) or the exocytosis blocker DD04107. V= Vehicle, Scr = Scrambled sequence of peptide DD04107, T= treatment. n=9. Each data point represents mean ± SEM. (*P<0.1, ***P<0.001, Mann Whitney test).

Figure 5. PAR₂ sensitizes TRPV1 in BDL nociceptors. (A) Representative traces of changes in FURA2-fluorescence indicative of Ca²⁺ influx upon a 0.1 μM capsaicin (0.1 Caps) pulse, expressed in arbitrary units (a.u.), in sham (black) or BDL (red) nociceptors exposed to PAR₂-Antg (*dashed line*) or Vehicle (*solid trace*). All neurons show a typical Ca²⁺-rise in response to raising extracellular [K⁺] to 40 mM. Neurons from sham-operated controls produced smaller capsaicin (Caps) responses than those from BDL rats. PAR₂-inhibition (PAR₂-Antg) suppressed Caps-responses in BDL neurons more strongly than in control neurons. (B) Mean FURA2-fluorescence changes induced by 0.1 Caps obtained like in (A) following different PAR₂-treatments in BDL and sham nociceptors. Veh= vehicle, Antg= PAR₂-Antg, AP= PAR₂ activating peptide and RP= a retroactive peptide as a negative control. (C) Percentage of K⁺-responsive neurons that also react to capsaicin at 0.1 μM. n (paired cultures) = 3. (D) Representative traces of capsaicin-induced Ca²⁺-responses as reported by FURA2-fluorescence at different agonist concentrations in BDL neurons (solid trace) compared to sham neurons (dashed line). (E) Mean peak FURA2-fluorescence magnitude obtained like in (D) with different capsaicin concentrations in BDL and

sham nociceptor cultures (black and white columns, respectively). **(F)** Proportion of capsaicin-responsive sham and BDL neurons in culture at different capsaicin concentrations. Each data point represents mean \pm SEM. (n.s. non significance, * $P < 0.1$, ** $P < 0.01$, *** $P < 0.001$, Mann Whitney test).

Figure 6. Changes in PAR₂ and TRPV1 protein expression induced in BDL rats. **(A)** Representative merged images from immunohistochemical detection of TRPV1 (red), PAR₂ (green) and overlay (yellow) in sham (left) and BDL DRG sections (right). The number of cells expressing both TRPV1 and PAR₂ was robustly increased in BDL rats. **(B)** Representative Western blots of TRPV1 and PAR₂ protein in plasma membrane and cytosolic fractions from sham and BDL DRG cultures obtained by cell surface biotinylation. Optical band densities were analyzed and normalized to cytosolic β -actin (right). Averages from four independent experiments are shown. **(C)** Merged images showing red-labeled TRPV1 together with CGRP (top), IB4 (middle) or NF200 (bottom) labeled in green. Co-localization results in yellow color. Scale Bar: 50 μ m. **(D-E)** Area frequency distribution of TRPV1⁺CGRP⁺ and TRPV1⁺NF200⁺ neurons, respectively. N (pairs) = 3. Each data point represents mean \pm SEM. (n.s. non significance, * $P < 0.1$, Mann Whitney test).

Table 1. Serum biomarkers of bilirubin (BR), alkaline phosphatase (AP), glutamic oxaloacetic transaminase (GOT) and glutamic pyruvic transaminase (GPT) obtained 7 days after surgery. Results are expressed as mean±SEM with (**P<0.01, n=5, Mann Whitney test).

Groups	BR (mg/dl)	AP (U/l)	GOT (U/l)	GPT (U/l)
Sham	0.14 ± 0.01	601.5 ± 59.5	84.8 ± 4.4	57.4 ± 1.2
BDL	6.43 ± 1.35**	1018 ± 46.6**	210.7 ± 27.2**	109.5 ± 14.3**

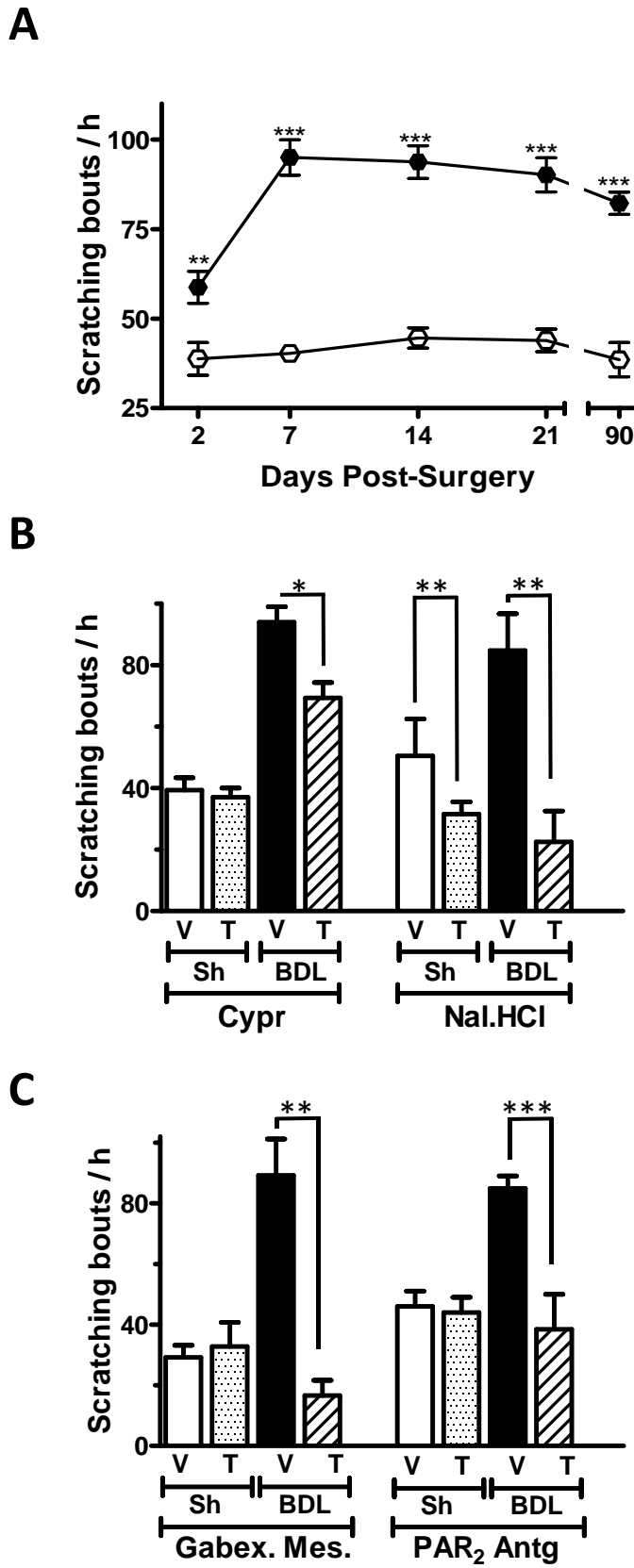


Figure 1

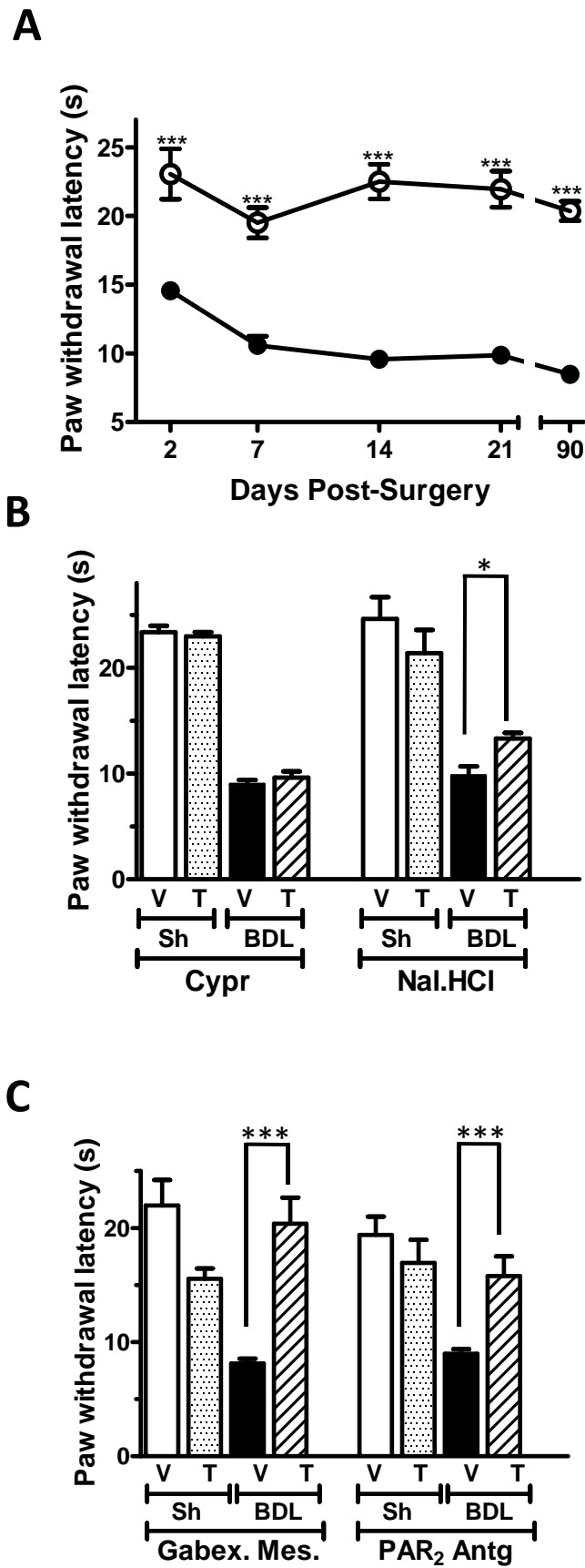


Figure 2

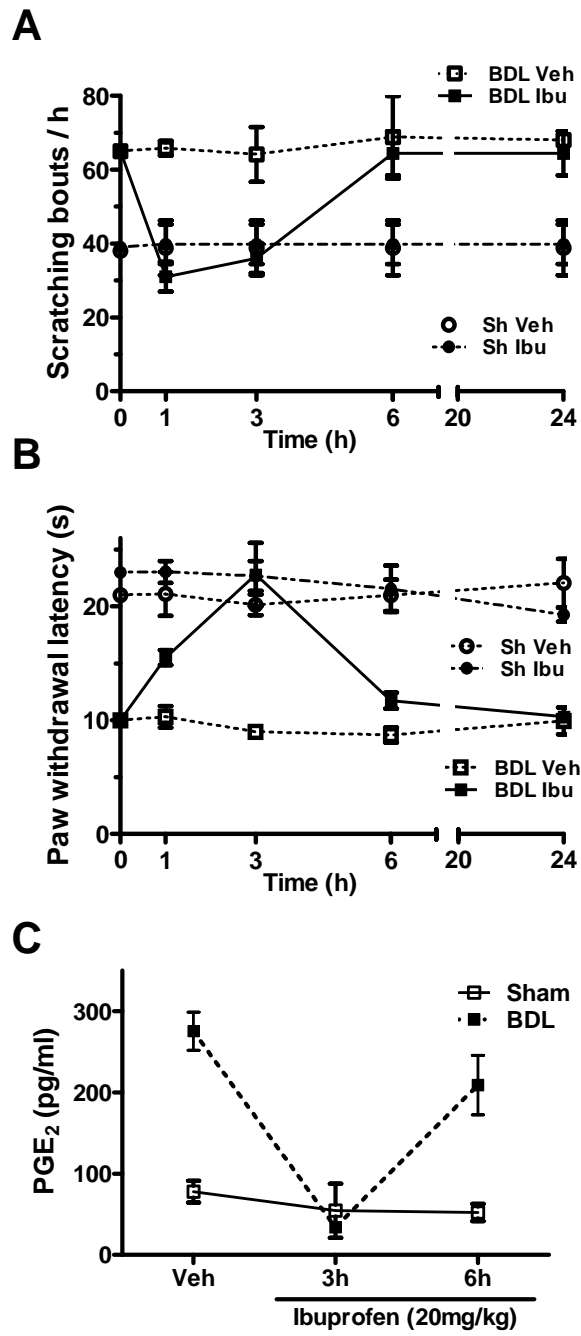


Figure 3

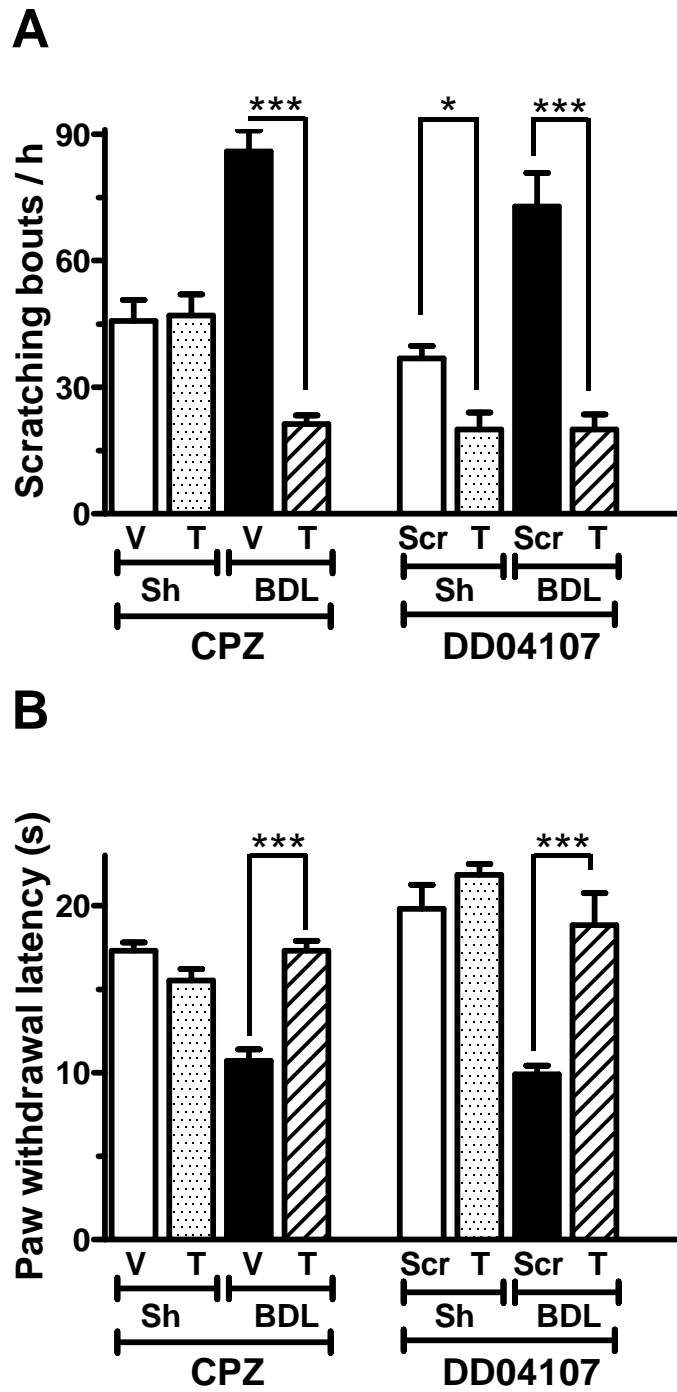


Figure 4

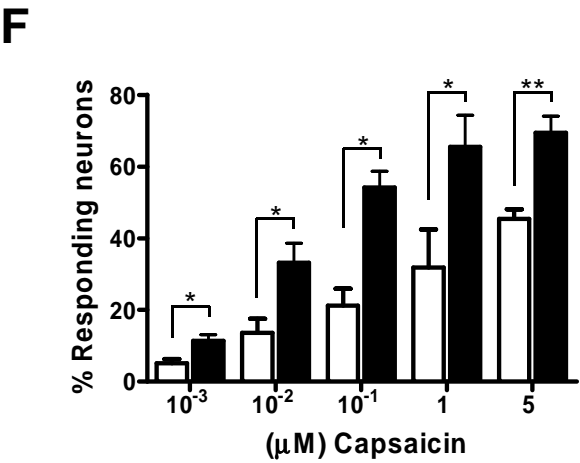
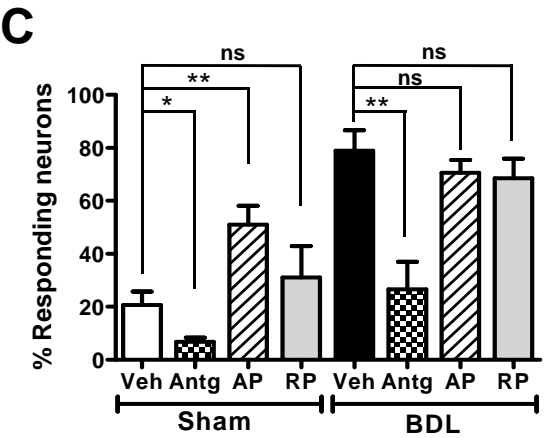
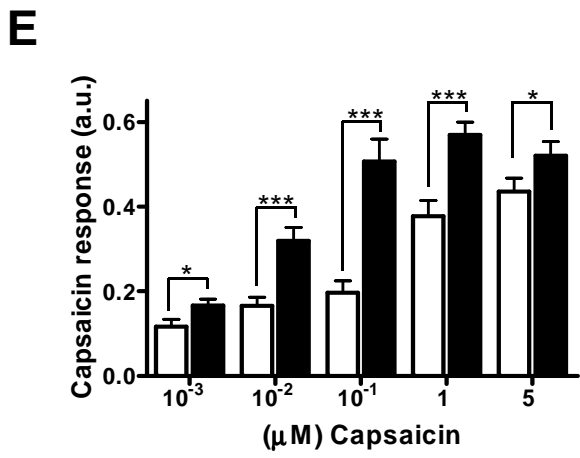
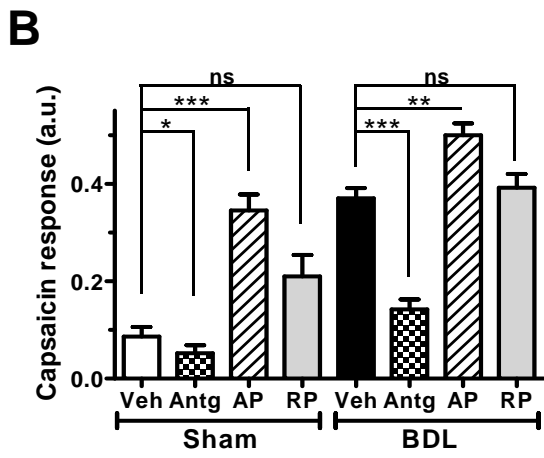
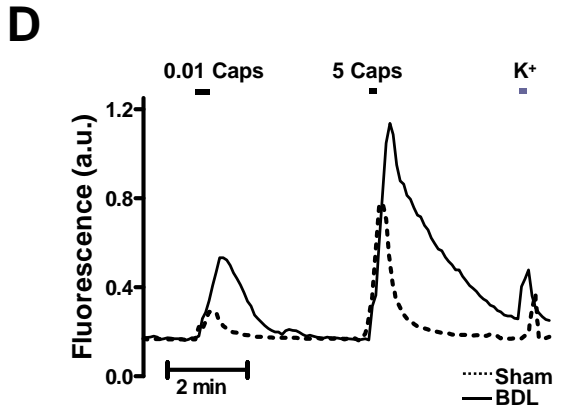
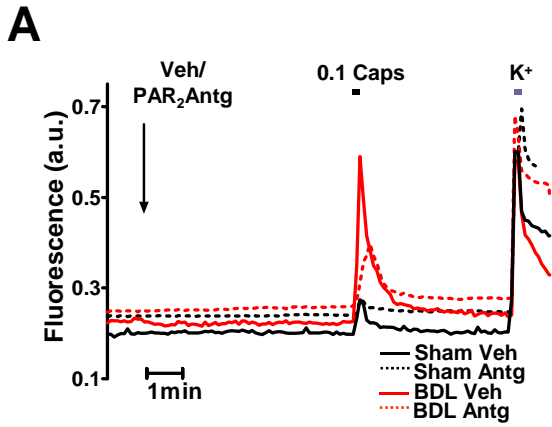


Figure 5

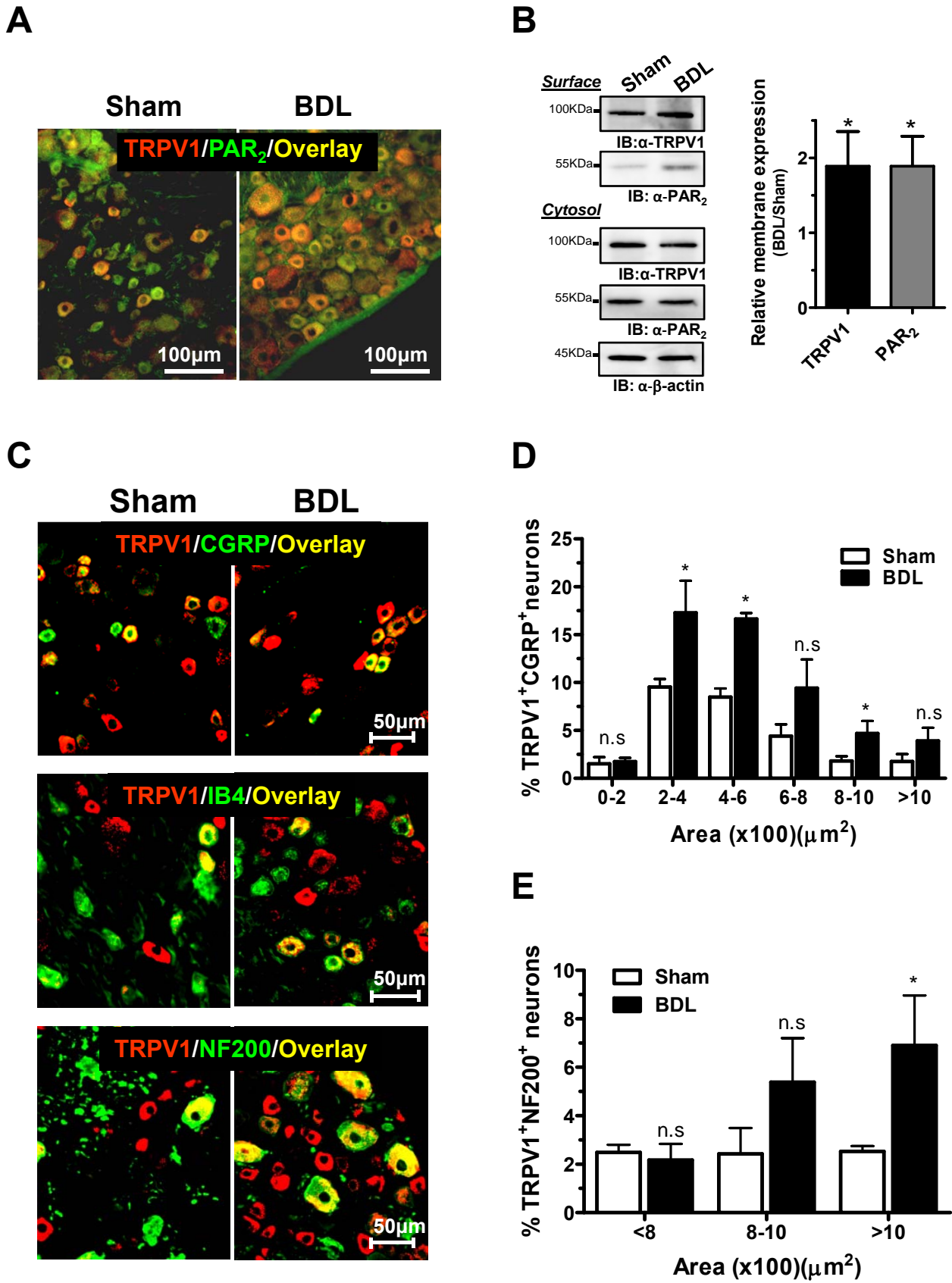
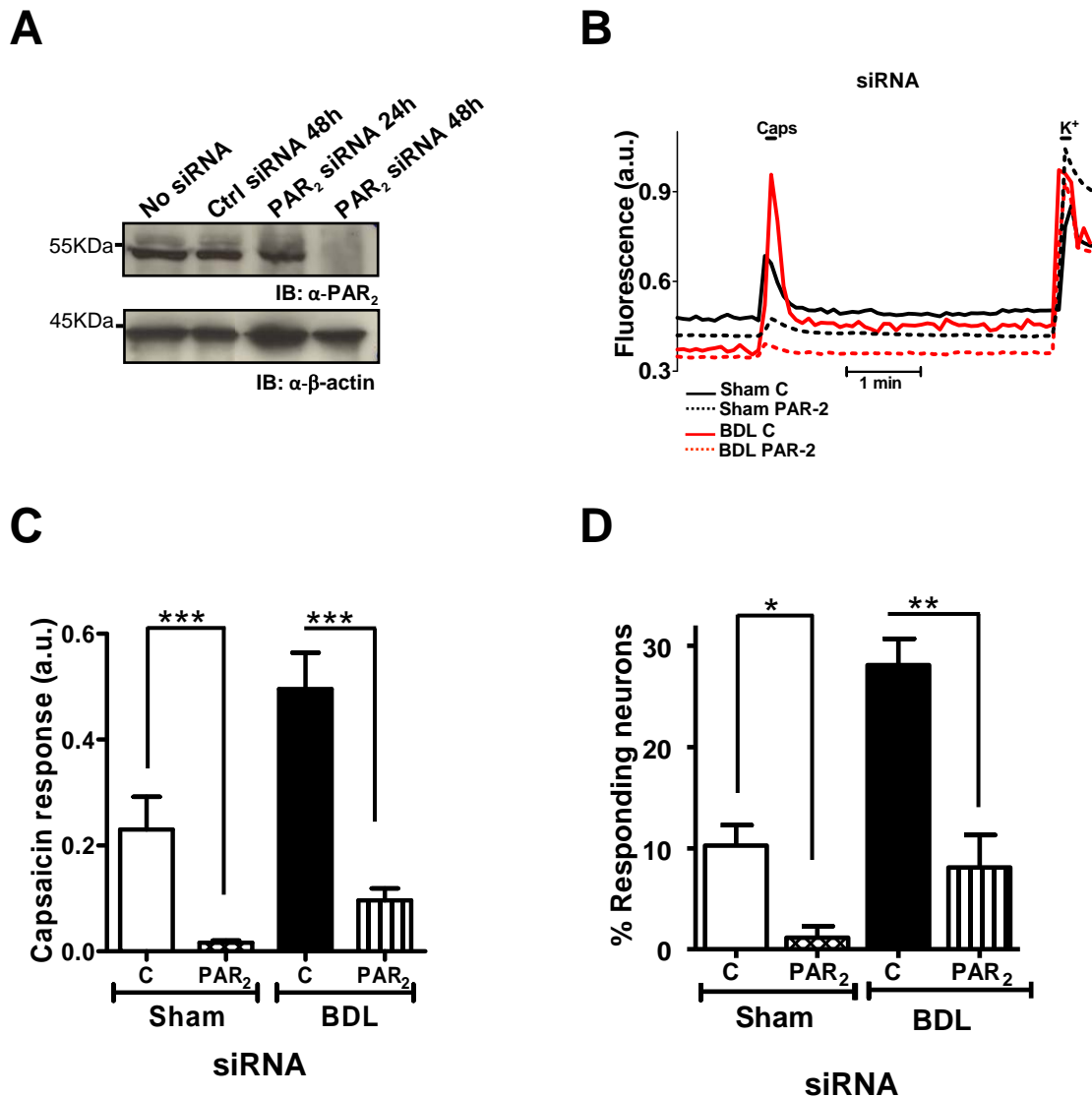
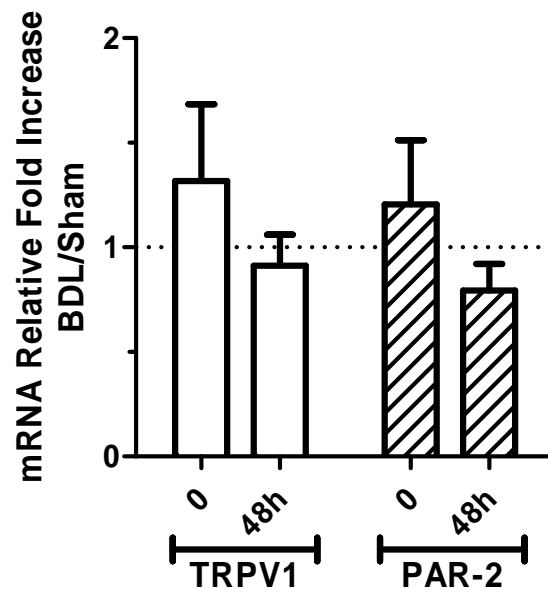


Figure 6

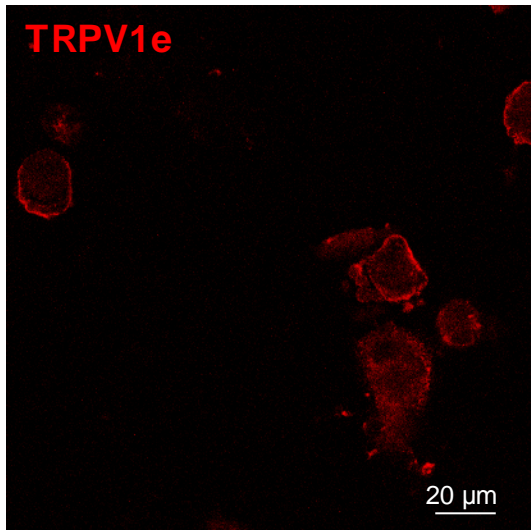


Supplementary Figure 1. Silencing of PAR2 reduces TRPV1 activity in both sham and BDL nociceptors. **(A)** Representative western blot of PAR₂ specific or control (Ctrl) siRNA transfected nociceptor neurons collected at 24 or 48h after transfection. **(B)** Traces of capsaicin-induced Ca²⁺ influx in sham- and BDL-neurons silenced with PAR2 (dashed lines) or Control (C) siRNA (solid traces). Cy3-labeled siRNA was used to select transfected cells. **(B)** Mean amplitude of capsaicin-induced Ca²⁺ influx and **(C)** percentage of responding neurons obtained upon control- and PAR2-silencing in Sham and BDL primary DRG cultures. n (paired cultures)=3.

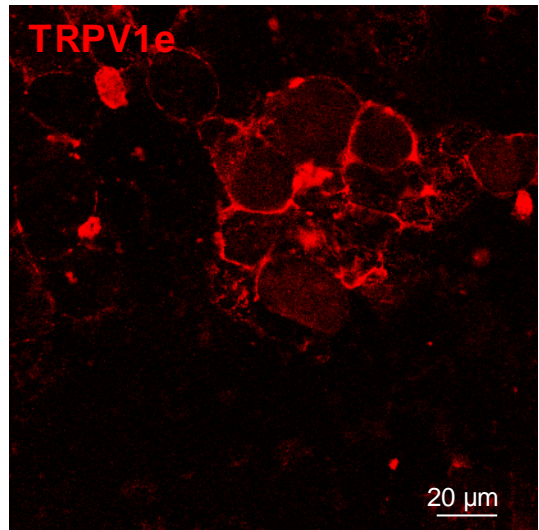


Supplementary Figure 2. Quantitative real-time PCR of PAR2 and TRPV1 expression in acutely dissected (0h) and after 2DIV cultures (48h). The results were normalized to GAPDH and the comparative threshold cycle (CT) method was used to calculate the relative expression. Each column represents the mean \pm S.E.M. of at least 4 independent experiments.

Sham



BDL



Supplementary Figure 3. Non-permeabilized live cell membranes from paired Sham and BDL rat primary DRG cultures maintained 12h *in vitro* were immuno-labelled with anti-TRPV1e (23) 1h at 4°C, then washed three times with cold PBS, fixed and then surface receptors stained with a red-labelled secondary antibody at 4°C. *Bar*, 20 μ m.

SUPPLEMENTARY EXPERIMENTAL PROCEDURES

PAR-2 silencing in primary cultures of dorsal root ganglion (DRG)

neurons

For silencing PAR2, 40pmol of Cy3-labeled Silencer® PAR2 and control siRNA (Applied Biosystems, Carlsbad, CA) were transfected by calcium phosphate precipitation. To validate the Cy3-labeled PAR₂ siRNA, cells were collected 24 and 48h after transfection and total protein extract was used for western blotting.

Quantification of PAR2 and TRPV1 RNA expression by Real-time Reverse Transcription (qPCR) from DRGs

Total RNA was collected by the Trizol method from acutely dissected and primary DRG cultures maintained 48 h in vitro. qPCR was performed using appropriate Taqman® (Applied Biosystems) and RNA-direct SYBR Green RT-PCR Master Mix. PAR2 and TRPV1 expression relative to a housekeeping gene (GAPDH) was determined by the change in cycle threshold (Δ Ct) method.

Measurement of DRG size

Images of DRG sections viewed with a Leica fluorescence microscope were captured using the same settings and exposure times for both sham and BDL samples. More than 5 sections per animal, N=3 pairs, >1000 total neurons per phenotype were analyzed.

Area measurement was obtained using Image J (NIH, Bethesda) by tracing the soma perimeter on a computer screen in a calibrated image. Statistical analyses were performed using non-parametric Mann-Whitney test.

Immunofluorescence of membrane TRPV1 in DRG cultures

Surface TRPV1 receptors of live cells in DRG primary cultures maintained 12h *in vitro* were labelled 1 h at 4°C with an antibody recognizing an extracellular epitope of the receptor, α -TRPV1e (1:1000, Alomone, Jerusalem, Israel). After washing in cold PBS, cells were fixed with cold 4% PFA. After washing, receptors were stained with an A568-secondary antibody, mounted, and analyzed by confocal microscopy (Leica TCS; Leica Microsystems, Wetzlar, Germany).